Green Chemistry

PAPER

View Article Online
View Journal | View Issue

Cite this: *Green Chem.*, 2025, **27**, 4750

Biomass–formic acid–hydrogen conversion process: sustainable production of formic acid from biomass using greenhouse gas†

Ju-Hyoung Park,[a] Young-Hoon Noh,[a] Jin Sung Kim,[a] Gyu-Seob Song,[a] Se-Joon Park,[b] Jong Won Choi,[c] Young-Chan Choi[a] and Young-Joo Lee*[a]

Sustainable green hydrogen production processes and efficient hydrogen storage methods are highly sought after to advance the hydrogen economy. Recently, a biomass–formic acid–hydrogen conversion process, which combines the formic acid production process from biomass with a formic acid dehydrogenation process, has been developed to address the two critical issues in the hydrogen field. Traditionally, inorganic acid reactants have been used to increase formic acid production during biomass treatment. In this study, we utilized a greenhouse gas as a heterogeneous acid reactant to replace toxic strong acid reactants. A formic acid yield of 36.18% was achieved using lignocellulose biomass under 30 bar CO_2 pressure, with 11 wt% H_2O_2 at 170 °C for 3 h, which is comparable to the yields reported in biomass conversion studies employing sulfuric acid, highlighting the competitiveness of this greener approach. We used a carbonic acid reactant instead of inorganic acid reactants, advancing the development of a sustainable formic acid production process. Various herbaceous biomass types (corn and wheat stover) were tested in the hydrolysis–oxidation system using CO_2 gas and H_2O_2. Formic acid yields (17.43 and 20.45%) were lower when herbaceous biomass was used than when red pine was used. Finally, formic acid derived from biomass was converted to hydrogen gas in a dehydrogenation system using a Pd heterogeneous catalyst at room temperature. This process eliminates the use of harmful inorganic acids while contributing to significant carbon reduction. Carbon emission analysis results show that this process can achieve a net carbon reduction of 5.83 tons of CO_2 per ton of hydrogen produced. This approach not only supports carbon-neutral hydrogen production but also demonstrates high scalability potential, making it a viable solution for meeting global sustainability targets at an industrial scale.

Received 31st December 2024,
Accepted 31st March 2025

DOI: 10.1039/d4gc06611a

rsc.li/greenchem

Green foundation

1. This study pioneers a carbon-neutral biomass-to-hydrogen process that utilizes CO_2 as a catalyst, replacing conventional inorganic acids. By integrating hydrolysis–oxidation with CO_2 and hydrogen peroxide, this method enhances formic acid yield while significantly reducing environmental impacts, providing a scalable pathway for green hydrogen production and storage.
2. The proposed process achieved a formic acid yield of 36.18% from red pine under optimized conditions (30 bar CO_2, 11 wt% H_2O_2, 170 °C, 3 hours). This yield is comparable to sulfuric acid-based processes but eliminates toxic acids, leading to a net carbon reduction of 5.83 tons of CO_2 per ton of hydrogen produced, outperforming traditional hydrogen carriers.
3. Further research could improve the purification of formic acid to enhance catalyst efficiency during dehydrogenation. Exploring renewable energy sources for process heating and optimizing biomass feedstock utilization could elevate the sustainability of this innovative approach.

Introduction

Hydrogen, a sustainable and eco-friendly energy carrier, allows for the highly efficient generation of electricity in power generation systems, including polymer electrolyte membrane fuel cells, in the foreseeable future.[1–5] However, two key issues must be addressed to enhance hydrogen utilization.[6] First, hydrogen is still primarily produced from fossil fuels, such as natural gas, coal, and oil, through processes like gasification,

[a]*Clean Air Research Department, Korea Institute of Energy Research (KIER), 71-2, Jang-dong, Yuseong-gu, Daejeon 305-343, Republic of Korea*
[b]*Technology Commercialization Team, Korea Institute of Energy Research (KIER), 71-2, Jang-dong, Yuseong-gu, Daejeon 305-343, Republic of Korea*
[c]*Energy Convergence System Research Department, Korea Institute of Energy Research (KIER), 71-2, Jang-dong, Yuseong-gu, Daejeon 305-343, Republic of Korea*
†Electronic supplementary information (ESI) available. See DOI: https://doi.org/10.1039/d4gc06611a

steam reforming, and auto-thermal reforming.[7–15] This dependence on fossil fuels must be overcome because it leads to significant environmental problems.[15,16] The development of cleaner, more efficient, and sustainable methods for hydrogen production from renewable resources is required.[17–20] Efficient hydrogen production using renewable resources such as biomass can undoubtedly contribute to the implementation of a hydrogen economy and help mitigate environmental problems.[15] In theory, biomass is a CO_2-neutral resource, as it is derived from CO_2 and water in nature through photosynthesis.[21–24] Additionally, it offers noteworthy advantages in terms of sustainability, availability, and diversity.[25] Various production strategies, including thermochemical and biological processes, are available for hydrogen conversion using biomass.[15,18,26] However, these methods are energy-intensive (low energy efficiency), require harsh conditions (high temperature and pressure), and have high operational costs. Moreover, they necessitate downstream purification of the produced gas to eliminate inhibitors such as CO, tar, ash, and nitrogen/sulfur-containing components.[27,28] Therefore, developing a cleaner, more efficient, practical, and economical process for hydrogen production using biomass is highly desirable and remains a key challenge.[29]

Second, even though hydrogen can be produced from renewable resources (*e.g.*, biomass conversion processes and electrolysis *via* solar and wind power), stability and storage are significant challenges for advancing the hydrogen economy. Various proposed hydrogen storage methods, such as high-pressure gas containers, cryogenic liquid/gas containers, and solid metal hydrides, suffer from problems such as the low volumetric and gravimetric densities of hydrogen, high pressure (700–800 bar) or low temperature (−252 °C) requirements, high security and energy demands, and hydrogen loss during storage.[30] Therefore, on-demand hydrogen release from stable, appropriate chemical precursors, such as liquid organic hydrogen carriers (LOHCs), is highly desirable to overcome these problems. LOHCs are cheap, safe, and easy to manage. Additionally, they allow for long-term hydrogen storage, and hydrogen can be transported *via* existing petroleum-based infrastructure.[31,32] Formic acid, with a high hydrogen capacity of 4.4 wt% and 53 g L^{-1}, has attracted increasing interest as a promising LOHC.[33–41] However, the current commercial production of formic acid is mainly derived from fossil fuels such as methanol and CO through an energy-intensive high-pressure process.[42,43] Developing a formic acid production process from renewable resources is preferable to mitigate carbon emissions. Although a sustainable formic acid production process has recently been developed *via* the electrochemical reduction (hydrogenation) of CO_2 and hydrogen/water,[44] it is not energy efficient because CO_2 is kinetically and thermally stable, requiring significant energy input, expensive catalytic systems, and harsh conditions to convert to formic acid.[45–47] Fossil-derived formic acid dominates current production, with green-derived FA still limited to niche applications. Integrating biomass-based FA production can significantly increase the share of renewable FA in the market, addressing this imbalance.

The biomass–formic acid–hydrogen (BFH) conversion process was proposed as a combined process of biomass hydrolysis–oxidation treatment and formic acid dehydrogenation for the development of a sustainable hydrogen production/storage process by the research group at Xi'an Jiaotong University in 2018 and the Korea Institute of Energy Research (KIER) group in 2019 and 2021. Zhang *et al.*[15] reported hydrogen production with up to 95% yield from non-food biomass (wheat straw) using a one-pot, two-step reaction. In the first step, wheat straw was converted to formic acid in the presence of 0.7 wt% sulfuric acid, 30 bar oxygen gas, and 1 vol% dimethyl sulfoxide at 160 °C for 3 h. In the second step, the formic acid obtained from the biomass was reacted using a homogeneous iridium reactant at 90 °C. The KIER group proposed a low-temperature (170 °C) and low-pressure process (internal staring pressure: 0 bar) for hydrogen production starting from lignocellulose comprising: (1) the conversion of the CF solution *via* the HOHT of the biomass using a homogeneous reactant consisting of a 2 wt% sulfuric acid and 11 wt% H_2O_2 solution at 170 °C for 3 h, (2) the purification of the CF DF or LCF solution to remove the by-products (lignin, saccharides, furfural, 5-HMF, *etc.*), and (3) the dehydrogenation of the DF or LCF solutions using a heterogeneous Pd catalyst at room temperature.[48] In addition, a mechanocatalytic depolymerization step was introduced using an organic acid such as citric acid before the hydrolysis–oxidation step to replace the toxic mineral acids and improve the formic acid yield. This step can promote the production of formic acid by facilitating the contact between the substrate (biomass) and the homogeneous reactant (acid-oxidant) during the hydrolysis–oxidation step, as pretreatment decreases the molecular weight of the cellulose and hemi-cellulose.[49]

Herein, we propose an efficient strategy for producing formic acid as an LOHC from various types of biomass (lignocellulose and herbaceous biomass) as sustainable feedstock, using CO_2 as an acid reactant. The selection of red pine, corn stover, and wheat stover as biomass feedstocks reflects their global availability, diverse compositions, and established sustainability profiles. These materials are representative of lignocellulose and herbaceous biomass, offering insights into the feasibility of the proposed method across varied feedstocks. The hydrolysis–oxidation reaction in the presence of CO_2 and H_2O_2 increased the formic acid yield by 161% compared to the oxidation reaction alone. In addition, we achieved a formic acid yield comparable to that of conventional sulfuric acid processes by using carbon dioxide as an acid reactant to replace inorganic acids in the conversion of biomass.

To convert formic acid derived from biomass into hydrogen, a dehydrogenation catalytic reaction is required. While homogeneous catalysts exhibit high activity, their recovery remains challenging, limiting their practical applications. Since the development of a heterogeneous catalyst for formic acid dehydrogenation at Oxford University in 2011, extensive research has been conducted in this field. As a result, Pd-based heterogeneous catalysts have gained significant attention due to their superior stability and ability to suppress CO formation.

In this study, we employed a Pd/NH_2-OH-KIE-6 catalyst, which utilizes an NH_2-functionalized mesoporous silica support to maximize Pd nanoparticle dispersion and enhance catalyst stability. Using this Pd-based catalyst, we successfully achieved stable hydrogen generation at room temperature from formic acid solutions produced from various biomass sources.[2,3,50,51]

Overall, this CO_2-based biomass treatment method could help mitigate global warming. This process is scalable and implementable, potentially supporting the hydrogen economy by producing LOHC-grade formic acid at lower carbon and energy footprints. By replacing conventional hydrogen storage methods, this approach could reduce CO_2 emissions by an estimated 5.83 tons per ton of hydrogen produced, underscoring its role in advancing sustainable energy systems.

Experimental

We propose an environmentally friendly biomass-to-formic acid conversion process that replaces sulfuric acid with CO_2 as the acid reactant in the existing methods (Fig. 1).

Conversion of biomass to a lignin-free crude formic acid (LCF) solution using raw biomass and analytical methods

We used three types of biomass (red pine, corn stover, and wheat stover from Korea) for conversion to formic acid. Before the conversion, we analyzed the components (carbohydrates and lignin) of the raw biomass following the two-stage acid-hydrolysis procedures stipulated in the National Renewable Energy Laboratory (NREL) Laboratory Analysis Procedure (LAP),[52–55] and the results are summarized in Table 1. The initial hydrolysis was conducted for 1 h at 30 °C using a biomass–sulfuric acid solution (72 wt%) mixed at a solid (biomass)–liquid (72 wt% sulfuric acid) weight ratio of 1 : 10. In this step, the polymeric structures of cellulose and hemicellulose are broken down by high-concentration sulfuric acid and converted into polysaccharides. After the first stage of hydrolysis is completed, water is added to dilute the sulfuric acid concentration to 4 wt%. The secondary hydrolysis was conducted for 1 h at 121 °C using a biomass-diluted sulfuric acid solution (4 wt%) to convert the polysaccharides into monosaccharides. The liquid products among the two-stage acid–hydrolysates (glucose, xylose, arabinose, galactose, acetic acid, formic acid, levulinic acid, 5-(hydroxymethly)furfural (5-HMF), and furfural) were detected by high-performance liquid chromatography (HPLC 1200 infinity series, Agilent Technologies, USA) using a Bio-Rad Aminex HPX-87H organic acid column (300 × 7.8 mm, USA) with a refractive index (RI) detector (mobile phase: 5.0 mM sulfuric acid, flow rate: 0.5 mL min^{-1}, and column temperature: 60 °C) following the NREL-LAP. We quantified the composition of the carbohydrate using the results of the liquid concentration. The acid–soluble lignin of three types of biomass was measured using a UV-vis spectrophotometer at 320 nm. After the two-stage acid hydrolysis, the solid sample was filtered and then dried in an oven at 105 °C for 24 h. The dried solid sample was combusted in a muffle furnace at 575 °C for 16 h. The difference between the dried and combusted solid weights was taken as the acid-insoluble lignin content.

Gel permeation chromatography (GPC) analysis was performed to compare the molecular weight of lignocellulose (red

Table 1 Components of raw biomass as feedstock

	Glucan (wt%)	XMG[a] (wt%)	Arabinan (wt%)	Total lignin[b] (wt%)
Red pine	39.88 ± 1.26	21.07 ± 0.16	1.49 ± 0.1	33.75 ± 0.26
Corn stover	30.30 ± 0.73	18.71 ± 0.38	0.82 ± 0.04	13.85 ± 0.52
Wheat stover	31.42 ± 1.71	22.94 ± 0.42	1.00 ± 0.05	14.58 ± 0.44

[a] Xylan + Mannan + Galactan. [b] Acid insoluble + acid soluble lignin.

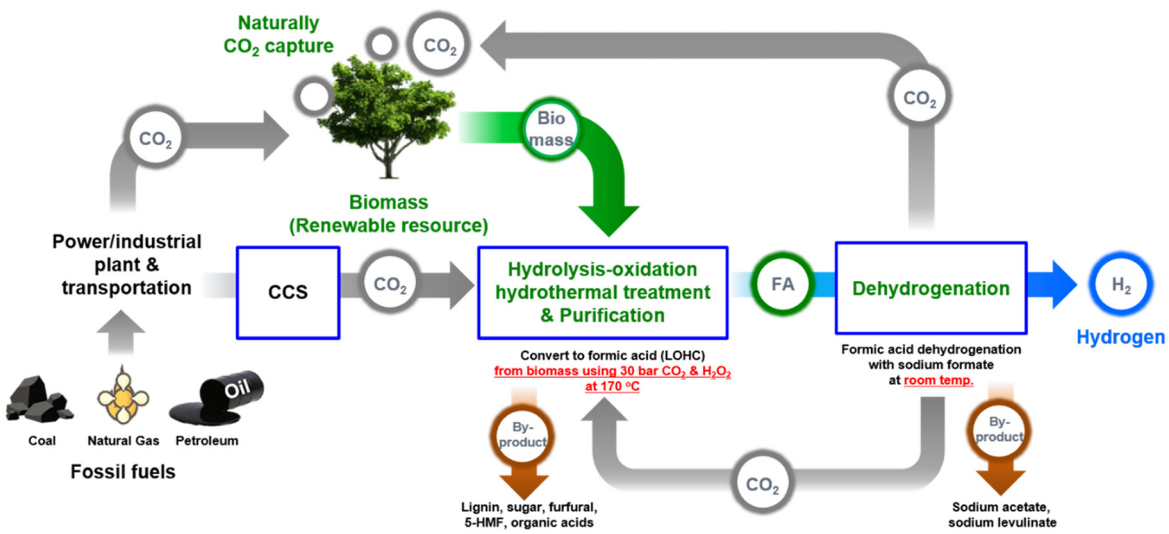

Fig. 1 Block diagram of a sustainable hydrogen production process from biomass using CO_2. CCS denotes carbon capture and storage.

pine) and the herbaceous biomass (corn stover and wheat stover).[49] Each biomass sample was dissolved in a 0.1 M $NaNO_3$ solution. The mixture was filtered using a 0.45 μm nylon filter. The $NaNO_3$-soluble product (flow rate: 1.0 mL min^{-1}, input volume: 200 μL) was analyzed using an HLC-8320 GPC system (Tosoh Co. Ltd) with columns (Tskgel guard PWxl + 2 × TSKgel GMPWxl + TSKgel G2500PWxl (7.8 mm × 300 mm)) at 40 °C using an RI detector.

Biomass (red pine, corn stover, and wheat stover, 600 μm, 10 g) and H_2O_2 (5.6, 11, or 16.8 wt% solutions, 78.96 g) were added to an autoclave reactor made of SUS 304 with an internal volume of 500 mL equipped with a stirring bar. These were mixed to homogeneity and sealed. The reactor was fitted with a small hole cap to connect to the CO_2 (99.9%; 10, 20, or 30 bar) gas cylinder, and the CO_2 gas was charged for 30 min in the reactor. After the loading procedure, the autoclave reactor was heated to the set-point temperature in an oil bath at a heating rate of 1 °C min^{-1} with stirring at 500 rpm at 150–190 °C for 1–4 h. To optimize the formic acid production process using CO_2 and H_2O_2, formic acid yield was evaluated under varying reaction conditions. A One-Factor-at-a-Time (OFAT) approach was employed, systematically adjusting one variable while maintaining the others constant. CO_2 pressure (10, 20, 30 bar), H_2O_2 concentration (5.6, 11, 16.8 wt%), reaction temperature (150, 170, 190 °C), and residence time (1, 2, 3, 4 h) were evaluated in sequential steps to determine their influence on formic acid production. All the experimental conditions are given in detail in Tables 2–4, and S1.† After the conversion of the biomass to the crude formic acid (CF) solution, the autoclave reactor was immediately soaked in a cooling water bath to stop the reaction. Finally, the CF solution was centrifuged at 3000 rpm for 30 min to remove lignin, and a lignin-free crude formic acid (LCF) solution was obtained. The LCF solution was distilled at 110 °C to remove the by-products, yielding a distilled formic acid (DF) solution.

All the liquid samples in the hydrolysis–oxidation product (LCF solutions) were also analyzed following the NREL-LAP. The formic acid yield from biomass was calculated using eqn (1).[48]

$$\text{Formic acid yield} = \frac{\frac{\text{FAc} \times \text{LCFSV}}{\text{FAmw}} \times n\text{FA}}{\frac{\text{BW} \times \text{XMGA}\%}{\text{XMGAmw}} \times n\text{XMGAC} + \frac{\text{BW} \times G\%}{\text{Gmw}} \times n\text{GC}} \times 100 \quad (1)$$

where, FAc is the formic acid concentration in the LCF solution (g L^{-1}), LCFSV is the LCF solution volume (L), FAmw is the formic acid molecular weight (46.03 g mol^{-1}), nFA is the number of carbon atoms in formic acid (1), BW is the mass of the raw biomass (g), XMGA% is the xylan + mannan + galactan

Table 2 Results of formic acid concentration and yield *via* hydrolysis–oxidation hydrothermal treatment (HOHT) of red pine by high-performance liquid chromatography (HPLC) with refractive index (RI) detector

Entry	Substrate	Acid reactant	Oxidant (H_2O_2) (wt%)	Temperature (°C)	Reaction time (h)	Formic acid (g L^{-1})	Formic acid yield (%)	Solid recovery yield (wt%)	Ref.
1[a]	—	CO_2 30 bar	11	170	3	—	—	—	—
2[b]	Red pine	—	—	170	3	0.56 ± 0.31	0.47 ± 0.26	71.33 ± 0.39	—
3[c]	Red pine	—	11	170	3	16.32 ± 0.29	13.85 ± 0.25	34.33 ± 0.18	—
4[d]	Red pine	CO_2 10 bar	—	170	3	1.73 ± 0.08	1.47 ± 0.07	70.00 ± 0.21	—
5[e]	Red pine	CO_2 10 bar	11	170	3	34.40 ± 0.98	29.20 ± 0.83	34.14 ± 0.09	—
6[f]	Red pine	CO_2 20 bar	11	170	3	39.16 ± 1.26	33.24 ± 1.07	33.96 ± 0.27	—
7[g]	Red pine	CO_2 30 bar	11	170	3	42.63 ± 0.30	36.18 ± 0.25	34.07 ± 0.33	—
8[h]	Red pine	CO_2 30 bar	11	170	1	29.25 ± 1.13	24.83 ± 0.96	—	—
9[i]	Red pine	CO_2 30 bar	11	170	2	31.58 ± 0.86	26.80 ± 0.73	—	—
10[j]	Red pine	CO_2 30 bar	11	170	4	30.04 ± 0.01	25.50 ± 0.01	—	—
11[k]	Red pine	CO_2 30 bar	11	150	3	25.03 ± 1.08	21.25 ± 0.92	—	—
12[l]	Red pine	CO_2 30 bar	11	190	3	18.97 ± 0.28	16.10 ± 0.24	—	—
13[m]	Red pine	CO_2 30 bar	5.6	170	3	13.72 ± 0.99	11.64 ± 0.84	—	—
14[n]	Red pine	CO_2 30 bar	16.8	170	3	18.30 ± 0.06	15.53 ± 0.05	—	—
15[o]	Red pine	Sulfuric acid 1 wt%	11	170	3	17.62 ± 0.25	16.50 ± 0.25	—	48
16[p]	Red pine	Sulfuric acid 2 wt%	11	170	3	39.23 ± 0.38	36.73 ± 0.38	—	48
17[q]	Red pine	Sulfuric acid 3 wt%	11	170	3	38.62 ± 0.61	36.23 ± 0.61	—	48

[a] Reaction condition: carbon dioxide 30 bar, and 78.96 g moisture for 3 h at 170 °C. [b] Reaction condition: 10 g of raw red pine, and 78.96 g moisture for 3 h at 170 °C. [c] Reaction condition: 10 g of raw red pine, and H_2O_2 11 wt% 78.96 g solution for 3 h at 170 °C. [d] Reaction condition: 10 g of raw red pine, carbon dioxide 10 bar, and 78.96 g moisture for 3 h at 170 °C. [e] Reaction condition: 10 g of raw red pine, carbon dioxide 10 bar, and H_2O_2 11 wt% 78.96 g solution for 3 h at 170 °C. [f] Reaction condition: 10 g of raw red pine, carbon dioxide 20 bar, and H_2O_2 11 wt% 78.96 g solution for 3 h at 170 °C. [g] Reaction condition: 10 g of raw red pine, carbon dioxide 30 bar, and H_2O_2 11 wt% 78.96 g solution for 3 h at 170 °C. [h] Reaction condition: 10 g of raw red pine, and carbon dioxide 30 bar, H_2O_2 11 wt% 78.96 g solution for 1 h at 170 °C. [i] Reaction condition: 10 g of raw red pine, carbon dioxide 30 bar, and H_2O_2 11 wt% 78.96 g solution for 2 h at 170 °C. [j] Reaction condition: 10 g of raw red pine, carbon dioxide 30 bar, and H_2O_2 11 wt% 78.96 g solution for 4 h at 170 °C. [k] Reaction condition: 10 g of raw red pine, carbon dioxide 30 bar, and H_2O_2 11 wt% 78.96 g solution for 3 h at 150 °C. [l] Reaction condition: 10 g of raw red pine, carbon dioxide 30 bar, and H_2O_2 11 wt% 78.96 g solution for 3 h at 190 °C. [m] Reaction condition: 10 g of raw red pine, carbon dioxide 30 bar, and H_2O_2 5.6 wt% 78.96 g solution for 3 h at 170 °C. [n] Reaction condition: 10 g of raw red pine, carbon dioxide 30 bar, and H_2O_2 16.8 wt% 78.96 g solution for 3 h at 170 °C. [o] Reaction condition: 30 g of raw red pine, sulfuric acid 1 wt%, and H_2O_2 11 wt% 236.34 g solution for 3 h at 170 °C. [p] Reaction condition: 30 g of raw red pine, sulfuric acid 2 wt%, and H_2O_2 11 wt% 236.34 g solution for 3 h at 170 °C. [q] Reaction condition: 30 g of raw red pine, sulfuric acid 3 wt%, and H_2O_2 11 wt% 236.34 g solution for 3 h at 170 °C.

Table 3 Results of formic acid concentration and yield *via* hydrolysis–oxidation hydrothermal treatment (HOHT) of corn stover by high-performance liquid chromatography (HPLC) with refractive index (RI) detector

Entry	Substrate	Acid reactant	Oxidant (H_2O_2) (wt%)	Temperature (°C)	Reaction time (h)	Formic acid (g L^{-1})	Formic acid yield (%)
1[a]	Corn stover	—	—	170	3	1.55 ± 0.19	1.88 ± 0.23
2[b]	Corn stover	—	11	170	3	6.45 ± 0.17	7.84 ± 0.21
3[c]	Corn stover	30	—	170	3	1.89 ± 0.38	2.29 ± 0.46
4[d]	Corn stover	30	11	170	3	14.34 ± 0.98	17.43 ± 1.19
5[e]	Corn stover	Sulfuric acid 2 wt%	11	170	3	15.41 ± 0.26	18.73 ± 0.32
6[f]	Ash extracted corn stover	30	11	170	3	14.23 ± 0.37	17.29 ± 0.45

[a] Reaction condition: 10 g of raw corn stover, and 78.96 g moisture for 3 h at 170 °C. [b] Reaction condition: 10 g of raw corn stover, and H_2O_2 11 wt% 78.96 g solution for 3 h at 170 °C. [c] Reaction condition: 10 g of raw corn stover, carbon dioxide 10 bar, and 78.96 g moisture for 3 h at 170 °C. [d] Reaction condition: 10 g of raw corn stover, carbon dioxide 30 bar, and H_2O_2 11 wt% 78.96 g solution for 3 h at 170 °C. [e] Reaction condition: 10 g of raw corn stover, sulfuric acid 2 wt%, and H_2O_2 11 wt% 78.96 g solution for 3 h at 170 °C. [f] Reaction condition: 10 g of raw corn stover, carbon dioxide 30 bar, and H_2O_2 11 wt% 78.96 g solution for 3 h at 170 °C.

Table 4 Results of formic acid concentration and yield *via* hydrolysis–oxidation hydrothermal treatment (HOHT) of wheat stover by high-performance liquid chromatography (HPLC) with refractive index (RI) detector

Entry	Substrate	Acid reactant	Oxidant (H_2O_2) (wt%)	Temperature (°C)	Reaction time (h)	Formic acid (g L^{-1})	Formic acid yield (%)
1[a]	Wheat stover	—	—	170	3	0.64 ± 0.01	0.72 ± 0.01
2[b]	Wheat stover	—	11	170	3	11.79 ± 0.54	13.23 ± 0.61
3[c]	Wheat stover	30	—	170	3	2.43 ± 0.05	2.73 ± 0.06
4[d]	Wheat stover	30	11	170	3	18.22 ± 0.67	20.45 ± 0.75
5[e]	Wheat stover	Sulfuric acid 2 wt%	11	170	3	18.75 ± 0.39	21.05 ± 0.44

[a] Reaction condition: 10 g of raw wheat stover, and 78.96 g moisture for 3 h at 170 °C. [b] Reaction condition: 10 g of raw wheat stover, and H_2O_2 11 wt% 78.96 g solution for 3 h at 170 °C. [c] Reaction condition: 10 g of raw wheat stover, carbon dioxide 30 bar, and 78.96 g moisture for 3 h at 170 °C. [d] Reaction condition: 10 g of raw wheat stover, carbon dioxide 30 bar, and H_2O_2 11 wt% 78.96 g solution for 3 h at 170 °C. [e] Reaction condition: 10 g of raw wheat stover, sulfuric acid 2 wt%, and H_2O_2 11 wt% 78.96 g solution for 3 h at 170 °C.

+ arabinan content in the raw biomass (wt%), *G%* is the glucan content in the raw biomass (wt%), XMGAmw is the molecular weight of C5 sugar (150.13 g mol^{-1}), Gmw is the molecular weight of C6 sugar (180.16 g mol^{-1}), *n*XMGAC is the number of carbon atoms in C5 sugar (5), and *n*GC is the number of carbon atoms in C6 sugar (6).

Preparation of formic acid dehydrogenation catalyst

The synthesis method of the formic acid dehydrogenation heterogeneous catalyst has been described in detail in previous reports from our group.[48,56–59]

Preparation of mesoporous silica (KIE-6)

A colloidal silica sol with a silica particle size of 5 nm was synthesized (base-catalyzed hydrolysis reaction) by refluxing a mixture that included a mixed solution of tetraethyl orthosilicate (TEOS) and ethanol added to an ammonia and water solution (TEOS : NH_3 : water : ethanol molar ratio = 1 : 0.084 : 53.6 : 40.7) under vigorous stirring at 50 °C for 3 h. The prepared silica sol (30 mL) was mixed with 4 g of glycerol and 0.4 g of sulfuric acid (10 wt% of added glycerol), and then the mixture was dried in a furnace at 150 °C for 24 h to eliminate the solvent and pre-carbonize the glycerol, affording the nanocomposite of silica nanoparticles and pre-carbonized carbon from glycerol. Subsequently, the mesoporous silica (KIE-6) was produced by calcining the dried sample in a furnace at 550 °C for 2 h.

Hydroxylation of mesoporous silica (OH-KIE-6)

We performed the hydroxylation of the mesoporous silica (OH-KIE-6) to increase the content of amine groups on the silica surface. A mixture of 1 g of KIE-6 and HCl 17.7 wt% solution was stirred at room temperature for 12 h. After the reaction, the mixture was separated into solid and liquid parts using a centrifuge system operated at 10 000 rpm for 5 min. The solid sample was washed with deionized (DI) water and separated three times until it was neutral. Finally, OH-KIE-6 was obtained after drying the separated solid sample under ambient conditions.

Amine-functionalization of hydrolyzed mesoporous silica (NH_2-OH-KIE-6)

OH-KIE-6 (1.5 g) and 3-aminopropyl trimethoxysilane (APTMS, 3.75 mL) were added to 150 mL of toluene, and the mixture was refluxed in a round-bottom flask at 110 °C for 3 h without stirring. After the amine-functionalization reaction, the mixture was filtered and washed to remove the unreacted APTMS. Finally, the filtered solid sample was dried at room temperature for 24 h to yield NH_2-OH-KIE-6.

Preparation of Pd catalyst for formic acid dehydrogenation (9 wt% Pd/NH_2-OH-KIE-6)

NH_2-OH-KIE-6 was used as a catalyst support to produce Pd catalysts for formic acid dehydrogenation. Palladium(II) nitrate hydrate (10 wt%, 0.0392 g) was mixed with 10 mL of DI water and stirred for 10 min. Then, the support was added to the mixture and stirred at room temperature for 6 h. Sodium borohydride ($NaBH_4$) (0.85 M, 2 mL) dissolved in the DI-water was added to the mixture under stirring at room temperature for 1 h to reduce Pd. Following the reaction, the mixture was centrifuged and washed. Finally, we obtained 9 wt% Pd/NH_2-OH-KIE-6 after drying the solid sample at room temperature.

Characterization of the 9 wt% Pd heterogeneous catalyst

To analyze the 9 wt% Pd catalyst supported on hydroxylated and amine-functionalized mesoporous silica, inductively coupled plasma (ICP)-atomic emission spectroscopy and X-ray photoelectron spectroscopy were performed using a Thermo Scientific iCAP 6500 duo ICP-emission spectrometer and a Kratos 165XP system, respectively (Table S2 and Fig. S1†).

Formic acid dehydrogenation using at room temperature

Before the dehydrogenation test, 0.68 g of sodium formate as an additive was dissolved in 15 mL of LCF or DF solution in a 30 mL glass vial and kept at room temperature for 3 h. The formic acid heterogeneous dehydrogenation catalyst (Pd/NH_2-OH-KIE-6, 0.055 g) was placed in a 100 mL Teflon-lined stainless steel autoclave reactor connected to a water-filled gas burette system and purged with nitrogen gas for 30 min. Then, the sodium formate LCF or DF solution was injected into the autoclave reactor using a syringe through a rubber septum to start the dehydrogenation reaction. The temperature was maintained at room temperature *via* a heater or air conditioner during the dehydrogenation period. During the dehydrogenation of formic acid, a gas mixture containing carbon dioxide and hydrogen is generated and transported through a pipeline from the reactor to a water-filled gas burette system (Fig. S2†). As the gas production increases, the water level in the graduated cylinder decreases. We monitored the decrease in water level and measured the gas volume in real-time. The presence of carbon dioxide and hydrogen in the formic acid dehydrogenation gas was confirmed through GC analysis. The GC analysis results are presented in the (Fig. S3†). After the dehydrogenation process, the catalyst was separated by centrifugation at 10 000 rpm for 5 minutes, washed five times with DI water, and then stored after air drying. However, catalyst reuse was not investigated in this study. The turnover frequency (TOF) was calculated according to eqn (2).[57]

$$\mathrm{TOF} = \frac{\mathrm{PV}}{\left(2RTn_{\mathrm{pd}}t\right)} \quad (2)$$

where P is the atmospheric pressure (101 325 Pa), V is the volume of the gas produced after 10 min of conversion, R is the universal gas constant (8.3145 m^3 Pa mol^{-1} K^{-1}), T is 298 K, n_{pd} is the mole number of Pd in the catalyst, and t is 10 min.

A life cycle analysis (LCA) and calculation of CO_2 emission

A life cycle analysis (LCA) was conducted to evaluate the environmental impact (carbon emission) of the biomass–formic acid–hydrogen (BFH) conversion process. The scope of the analysis includes biomass cultivation, hydrolysis–oxidation, formic acid distillation, and hydrogen production. The CO_2 emissions from each stage were quantified and compared with conventional hydrogen production methods. The carbon emissions from biomass conversion were estimated based on the energy consumption of the process, assuming that the required energy was supplied by liquefied natural gas (LNG) combustion. Additionally, CO_2 absorption by biomass growth was estimated using literature values for red pine. The detailed analysis is shown in ESI.†

Results and discussion

LCF solution production from various biomasses *via* hydrolysis–oxidation with CO_2 gas in the presence of H_2O_2

Achieving a higher formic acid yield is important because the formic acid conversion rate from biomass determines the overall hydrogen production and efficiency in the entire BFH process.[15,48] Various methods for formic acid production (pyrolysis, acid hydrolysis, catalytic oxidation, wet oxidation, *etc.*) from biomass have been researched using glucose, cellulose, and raw biomass.[60] Herein, we propose a new formic acid conversion process using biomass *via* HOHT in the presence of CO_2 (greenhouse gas) and H_2O_2 (Fig. 1). Before biomass test, in the reaction of carbon dioxide and hydrogen peroxide, it was not converted to an organic acid such as formic acid (Table 2, entry 1). First, it is well-known that the conversion of biomass to formic acid or to saccharides (sugars of 5 and 6 carbon atoms) *via* hydrothermal treatment is difficult without reactants (Table 2, entry 2; Table 3, entry 1; Table 4, entry 1).[61–63] Next, we compared the formic acid production yield when different reactants (CO_2 and oxidant) were used. A higher formic acid production yield was achieved when only an oxidant (red pine (Table 2, entry 3): 13.85%, corn stover (Table 3, entry 2): 7.84%, and wheat stover (Table 4 entry 2): 13.23%) was used compared to when only an acid reactant (red pine (Table 2, entry 4): 1.47%, corn stover (Table 3, entry 3): 2.29%, and wheat stover (Table 4, entry 3): 2.73%) was used. When reactants such as carbon dioxide and hydrogen peroxide are used alone, the conversion of formic acid is low.

When the reaction was performed in the presence of CO_2 and H_2O_2, the formic acid yield increased significantly (Table 2, entry 5: formic acid yield 29.20%), indicating that the co-existence of carbonic acid and oxidant was essential for the conversion of cellulose and hemi-cellulose into formic acid.

First, we investigated the effect of CO_2 pressure on the formic acid yield. Compared to 10 bar CO_2 (entry 5), the yield

of formic acid increased by up to 36.18% at 30 bar CO_2 (entry 7). We measured the pH of the carbonic acid solution for different CO_2 pressures. Starting at pH 7 in DI water, the pH decreased as the CO_2 pressure increased, reaching 6 at CO_2 pressures of 10 and 20 bar and 5 at a CO_2 pressure of 30 bar. Therefore, maintaining the pH value at 5 or lower is effective for the conversion of formic acid.

As the reaction proceeded, the formic acid yield gradually increased, reaching a peak value of 36.18% at 170 °C and 3 h, and then decreased (entries 7–12). In addition, Table 2, entries 7, 13, and 14, suggest that the oxidant concentration is an important parameter for the efficient production of formic acid from biomass, with the highest yields obtained when 11 wt% H_2O_2 was used. This indicates that an excess amount of oxidant could lead to the decomposition of the already converted formic acid into lower molecular weight compounds (ex. CO_2) than carboxylic acid (HCOOH), as shown in the liquid sample analysis results (Table S1†). The optimum conditions for formic acid production from biomass were determined to be 30 bar CO_2 and 11 wt% H_2O_2 reactants at 170 °C, with a reaction time of 3 h. Through this experiment, we established a biomass-based green formic acid production process by entirely replacing sulfuric acid with CO_2 (Table 2, entries 15–17). Fig. 2 shows the overall pathway for formic acid conversion from biomass *via* the hydrolysis–oxidation system in the presence of CO_2 and H_2O_2.[21,64–70] Formic acid is converted from cellulose and hemicellulose among the biomass components. These polymers have a highly crystalline structure and strong bonding; therefore, they must be converted into intermediate substances with low-molecular weight for conversion to formic acid. Acid-hydrolysis is well-known as a process that effectively destroys the biomass structure. In our proposed process, carbon dioxide is utilized. Carbon dioxide is partially dissolved in water to form carbonic acid (H_2CO_3), which acts as an acid by releasing H^+ ions ($H_2CO_3 \rightarrow H^+ + CO_3^{2-}$ or HCO_3^-).

The first known pathway is as follows. Carbonic acid dissolved in water breaks the β-1,4-glycosidic linkages of cellulose and hemicellulose to form hexose and pentose. The water-soluble hexose is then easily dehydrated by carbonic acid to produce 5-hydroxymethylfurfural (5-HMF). The 5-HMF is rehydrated by H^+ ions to produce levulinic acid and formic acid. It also releases formaldehyde and is converted to furfural during the decomposition process. Similarly, furfural is rehydrated to form formic acid. The pentose converted from hemicellulose is dehydrated and converted to furfural, and then finally converted to formic acid through the above reaction. The oxygen generated from hydrogen peroxide oxidizes levulinic acid to convert it into formic acid and acetic acid. Generally, when the α-carbon of levulinic acid is attacked and oxidation proceeds, the concentration of formic acid increases. Conversely, when the β-carbon is attacked, the concentration of acetic acid increases. According to our process analysis, since formic acid is the main product, it can be concluded that the α-carbon of levulinic acid is activated.

The second pathway involves the direct oxidation of hexose and pentose to formic acid. Hexose and pentose generated by carbonic acid are directly oxidized by oxygen supplied from hydrogen peroxide. When the α- and β-carbons are activated by oxygen, they are finally converted to formic acid.

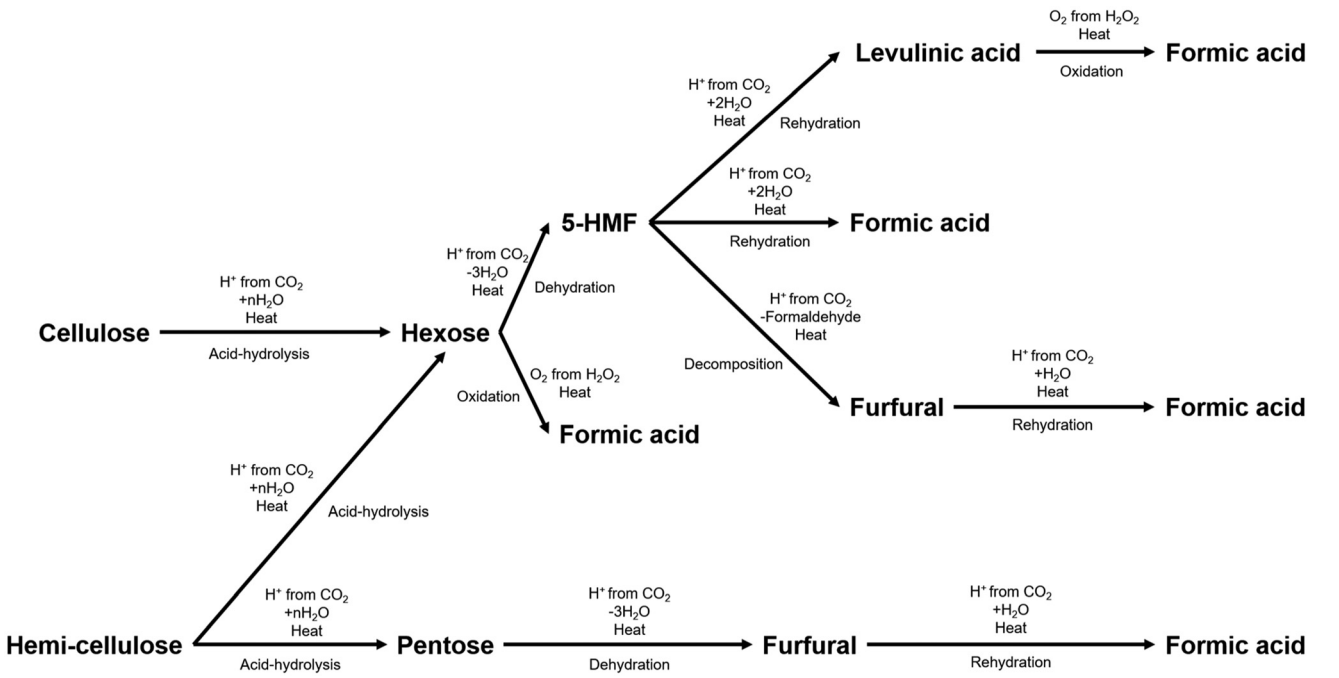

Fig. 2 Overall pathway for the production of formic acid from biomass components (cellulose, and hemi-cellulose) by HOHT in presence of CO_2 and H_2O_2.

We measured the solid recovery yield in several key variable experiments during the formic acid conversion experiments. After the reaction was completed, the solid phase was separated from the liquid, washed multiple times, dried, and then weighed (Fig. S4†). In the absence of reactants such as carbon dioxide and hydrogen peroxide, the solid recovery yield was 71.33% (Table 2, entry 2), indicating that most of the cellulose and hemi-cellulose were not converted into smaller units. In the reaction where only hydrogen peroxide was added, the solid recovery yield was 34.33% (Table 2, entry 3), which was similar to the lignin content of red pine. This suggests that cellulose and hemicellulose were converted into liquid-phase organic compounds by hydrogen peroxide. When 10 bar of carbon dioxide was introduced into the reaction, a high solid recovery yield of 70% (Table 2, entry 4) was observed. Although the solid recovery yield was slightly lower than in the absence of reactants, this result indicates that cellulose and hemi-cellulose still remained in polymeric form. When both carbon dioxide and hydrogen peroxide were present, the solid recovery yield was similar to the lignin content of red pine (Table 2, entries 5–7). This suggests that hydrogen peroxide is a key reactant in converting cellulose and hemicellulose into liquid-phase substances. However, the solid recovery yield alone cannot predict the formic acid yield. In the liquid phase, additional dehydration and oxidation reactions determine the final formic acid yield.

Different types of herbaceous biomasses were used as substrates to examine their applicability for formic acid production under the optimum conditions. When corn and wheat stover were used, the formic acid yield was 17.43% (Table 3, entry 4) and 20.45% (Table 4, entry 4), respectively. These formic acid yields imply that the sulfuric acid process has been completely replaced by a carbon dioxide-based process using a variety of biomass sources (Tables 3 and 4 entry 5). The formic acid yield of the hydrolysis–oxidation process increased compared to that of the oxidation system alone to 161.23% (using red pine), 106.03% (using corn stover), and 54.57% (using wheat stover).

To confirm the significant difference in formic acid yields, the degree of depolymerization of the biomass was measured, and the results for each biomass are shown in Table 5. M_w represents the weight-averaged molecular weight, and a larger M_w/M_n value indicates a wider molecular weight distribution of the polymer. Herbaceous biomass (corn stover and wheat stover) has a wider molecular weight distribution than woody biomass (red pine). The wider the molecular weight distribution of the polymer, the more difficult it is to decompose it into smaller molecules (oligomer, disaccharide, monosaccharide, and C1 or C2 chemicals). Therefore, under the same conditions, red pine is easily decomposed into formic acid, whereas corn stover and wheat stover are difficult to decompose into formic acid. However, because biomass maintains a complex chemical bonding structure with various components, it is difficult to predict the formic acid yield based only on the polymer distribution.

Therefore, we conducted additional experiments to relate the formic acid yield based on the component content of the biomass. Under the optimal reaction conditions, glucan (cellulose) is expected to have the greatest impact on the formic acid yield. Woody biomass generally has higher glucan levels compared to herbaceous biomass, and this compositional difference influences the formic acid yield. The relationship between biomass composition and formic acid yield can be used the eqn (3). The empirical correlation was derived based on experimental data obtained under the following conditions: biomass components (Table 1) and formic acid yield of optimal condition (carbon dioxide 30 bar), and H_2O_2 11 wt% solution for 3 h at 170 °C conditions, (red pine: Table 2 entry 7, corn stover: Table 3 entry 4, wheat stover: Table 4 entry 4). The relative error for empirical correlation with experimental data was less than 1% (ESI Table S3†).

$$Y = -44.03 + 1.90\times X_1 + 0.21\times X_2 + 0.13\times X_3 \quad (3)$$

where Y is the formic acid yield (%), X_1 is the glucan content (wt%), X_2 is the XMG content (wt%), and X_3 is the arabinan content (wt%).

To validate the formic acid yield empirical correlation based on biomass composition, we conducted formic acid conversion experiments using lignin (solid sample after complete hydrolysis of biomass using sulfuric acid solution), cellulose (reagent), and xylan (reagent). Lignin was not converted to formic acid in the proposed process (Table 6, entry 1). Therefore, the lignin content in biomass does not affect formic acid conversion and was excluded from the empirical correlation. Among the components, cellulose showed the highest conversion (Table 6, entry 2). Generally, the reaction rate of C5 polymers is faster than that of C6 polymers.[71] That

Table 5 Gel permeation chromatograph of the depolymerization of raw red pine, corn stover, and wheat stover biomass

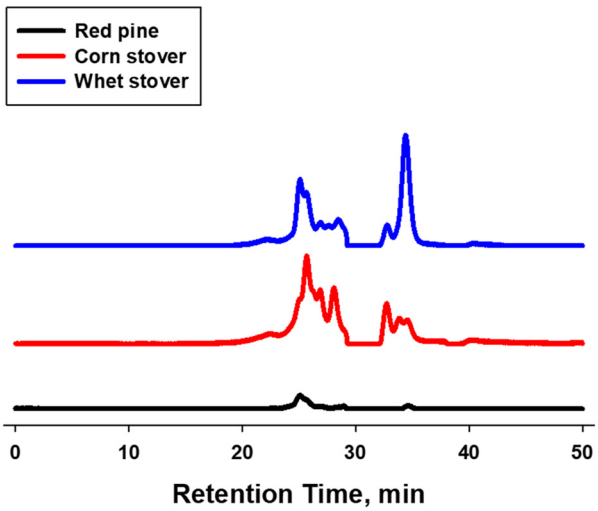

	Total M_w	Total M_w/M_n
Red pine	1552	1.21
Corn stover	7428	16.64
Wheat stover	3631	8.08

Table 6 Results of optimal hydrolysis–oxidation hydrothermal treatment (HOHT) of lignin, cellulose, and xylan by high-performance liquid chromatography (HPLC) with refractive index (RI) detector

Entry	Glucose (g L^{-1})	XMG[a] (g L^{-1})	Arabinose (g L^{-1})	Acetic acid (g L^{-1})	Levulinic acid (g L^{-1})	5-HMF (g L^{-1})	Furfural (g L^{-1})	Formic acid (g L^{-1})
1[b]	—	0.14	—	—	0.08	—	—	—
2[c]	17.20	—	0.20	4.72	1.87	0.72	4.32	27.50
3[d]	—	—	—	4.54	0.10	0.07	32.31	19.50

[a] Xylose + Mannose + Galactose. [b] Reaction condition: 10 g of lignin, carbon dioxide 30 bar, and H_2O_2 11 wt% 78.96 g solution for 3 h at 170 °C. [c] Reaction condition: 10 g of cellulose, carbon dioxide 30 bar, and H_2O_2 11 wt% 78.96 g solution for 3 h at 170 °C. [d] Reaction condition: 10 g of xylan, carbon dioxide 30 bar, and H_2O_2 11 wt% 78.96 g solution for 3 h at 170 °C.

is, under the same conditions, xylan quickly decomposed into pentose and was mostly converted to furfural (Table 6, entry 3). This reaction pathway shows that hydrolysis by carbonic acid is predominant over oxidation. In the xylan-based experiment, pentose was not present in the solution (Table 6 entry 3). In contrast, the reaction rate in the cellulose experiment was slower compared to that in the xylan experiment. A significant amount of undecomposed glucose remained in the solution, and further reaction (oxidation) with glucose resulted in a higher formic acid concentration and lower furfural concentration (Table 6, entry 2). In summary, under optimal conditions, xylan is rapidly converted to furfural through pentose, while cellulose is converted more slowly to hexose but is rapidly converted to formic acid through oxidation by oxygen. If the concentration of carbonic acid is increased, both xylan and cellulose can be converted more efficiently into formic acid, which aligns with the observed results of increased formic acid yield with higher CO_2 pressure (Table 2, entries 5–7).

Ebitani *et al.* demonstrated that formic acid can be synthesized from monosaccharides using hydrogen peroxide as an oxidant, achieving a high yield of 78% with Mg–Al hydrotalcite as a reusable catalyst.[72] Inspired by this research, we studied the influence of the metal components contained in biomass with hydrogen peroxide on formic acid conversion. Table 7 shows the ash content of raw corn stover and the types of metals present in the ash. The ash content of corn stover is quite high at 8.06 wt%, and the predominant metal in the ash is potassium (64.47 wt%). Typically, alkali metals in the ash are removed through acid (organic acids) treatment, while acidic metals such as SiO_2 are removed by base (NaOH) treatment. However, acid or base treatments can collapse the polymer structure of the biomass, making the metal components unsuitable as catalytic variables in formic acid conversion studies. Recent research indicates that alkali metals can be removed through a mechano-non-catalytic wet treatment process without the need for acid or base treatment.[25]

We mixed raw corn stover with DI-water in a 1 : 10 ratio and then pulverized it to remove the ash at room temperature, recovering the solid component. As shown in Table 7, the ash content decreased from 8.06 wt% to 1.64 wt% through this ash removal process, with most of the potassium being eliminated. Using the corn stover with most of the K removed, we compared the yield of formic acid production under the same process conditions (30 bar CO_2, 11 wt% hydrogen peroxide, 170 °C, 3 h conditions) (Table 3, entry 6). The formic acid yield from the K-removed corn stover was almost identical to that obtained using raw corn stover. Therefore, the alkali metals contained in the biomass do not significantly affect the formic acid conversion process.

Dehydrogenation of LCF and DF solutions derived from three types of biomasses using a Pd catalyst supported on NH_2-OH-KIE-6

We performed the dehydrogenation of LCF and DF solutions derived from red pine, corn stover, and wheat stover at room temperature using a Pd heterogeneous catalyst (Pd/NH_2-OH-KIE-6) with sodium formate as an additive. The characterization of the catalyst is provided in the ESI (Table S2 and Fig. S1†). The LCF solution from red pine was diluted from a formic acid concentration of 42.63 g L^{-1} (9.26 mmol) to 17.32 g L^{-1} (3.76 mmol) because the higher formic acid concentration solution was not suitable for the heterogeneous dehydrogenation system. According to previous research,[49] the higher concentration LCF solution (53.32 g L^{-1}, 91.47 mmol) was hardly converted to hydrogen, and the hydrogen conversion at 200 min was only 11.86%.

In the case of the dehydrogenation of the diluted LCF solution (17.32 g L^{-1}, 3.76 mmol) derived from red pine with a sodium formate additive, the gas production volume/conver-

Table 7 Ash and metal content of raw and ash extracted corn stover samples analyzed by proximate analysis and X-ray fluorescence (XRF)

	Ash wt%	Na_2O	MgO	Al_2O_3	SiO_2	P_2O_5	K_2O	CaO	TiO_2	MnO	Fe_2O_3
Raw corn stover	8.06	—	5.15	—	13.26	14.73	64.47	—	0.14	0.29	1.96
Ash extracted corn stover	1.64	—	4.12	1.82	61.15	14.59	2.41	11.84	0.21	0.20	3.65

sion at 200 min and TOF at 10 min were measured to be 172 mL/93.28% and 115.15 mol H_2 mol per catalyst per h, respectively (black line in Fig. 3). For the undiluted LCF solution (14.34 g L^{-1}, 3.12 mmol) derived from corn stover, the gas production volume/conversion at 200 min and TOF were measured to be 62 mL/40.60% and 28.79 mol H_2 mol per catalyst per h, respectively (black line in Fig. 4). They were 99 mL/51.03% and 80.61 mol H_2 mol per catalyst per h for the undiluted LCF solution (18.22 g L^{-1}, 3.96 mmol) derived from wheat stover (black line in Fig. 5). The catalytic activity (gas production volume, conversion, and TOF) of the raw solutions was very low. It was considered that the higher by-product (saccharides, 5-HMF, furfural, and unconfirmed organic components) concentration in the raw solution than in the diluted solution disturbed the contact between the catalyst and reactant (formic acid). The formic acid/by-product ratios are summarized in Table 8, and the relationship between this ratio and formic acid production yield is shown in Fig. 6. As the formic acid/by-product ratio increases, the formic acid yield also increases. However, when the amount of biomass-derived by-products is higher, the catalytic active sites are contaminated, leading to a decrease in conversion efficiency.

Therefore, we conducted an additional dehydrogenation test after the distillation process at 110 °C to enhance the catalytic activity. The concentrations of the DF solutions from red pine, corn stover, and wheat stover were 15.69 g L^{-1} (3.41 mmol), 13.52 g L^{-1} (2.94 mmol), and 14.26 g L^{-1} (3.10 mmol), respectively (Table 9). Based on the results of this

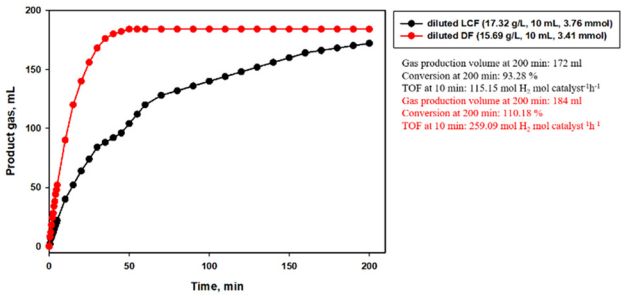

Fig. 3 Results of the dehydrogenation of the diluted LCF and DF solutions derived from red pine with sodium formate at room temperature.

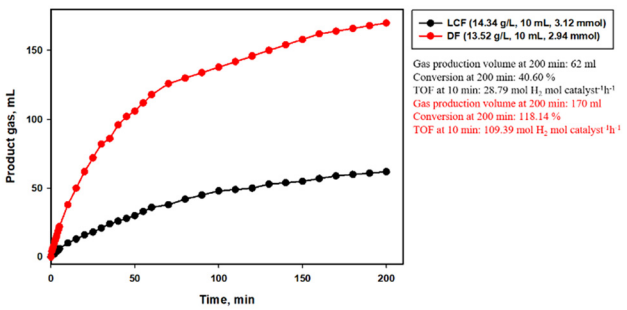

Fig. 4 Results of the dehydrogenation of the LCF and DF solutions derived from corn stover with sodium formate at room temperature.

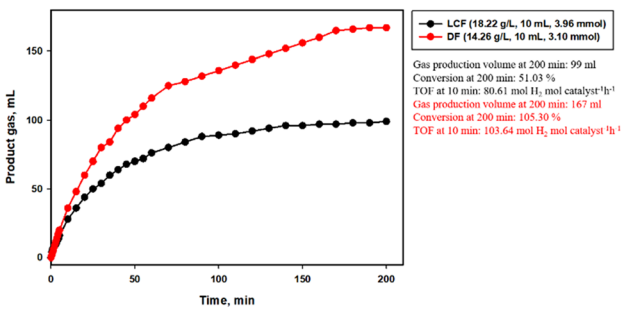

Fig. 5 Results of the dehydrogenation of the LCF and DF solutions derived from wheat stover with sodium formate at room temperature.

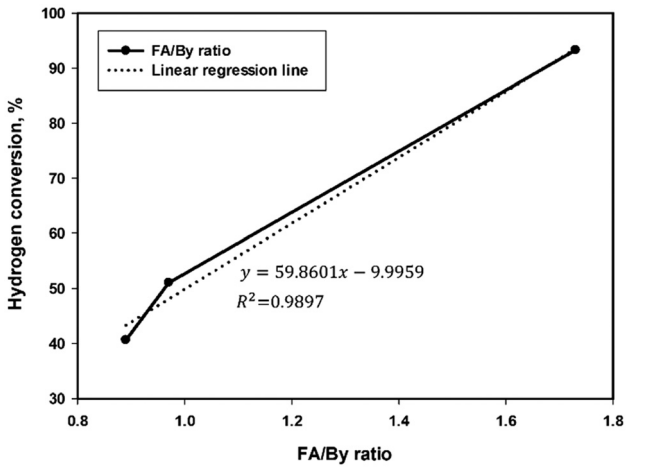

Fig. 6 Comparison of the effects of formic acid and by-products ratio in CF solution on hydrogen conversion rate.

Table 8 Concentration of various LCF solution by high-performance liquid chromatography (HPLC) with refractive index (RI) detector and by-product/formic acid ratio

Entry	Glucose (g L^{-1})	XMG[a] (g L^{-1})	Arabinose (g L^{-1})	Acetic acid (g L^{-1})	Levulinic acid (g L^{-1})	5-HMF (g L^{-1})	Furfural (g L^{-1})	Formic acid (g L^{-1})	Formic acid/By product ratio
1[a]	1.27	0.79	0.32	5.06	1.71	0.59	0.28	17.32	1.73
2[b]	2.33	1.12	0.75	9.52	0.46	0.74	1.22	14.34	0.89
3[c]	3.90	1.63	0.92	9.28	0.37	0.84	1.91	18.22	0.97

[a] Diluted LCF solutions from red pine. [b] Raw LCF solutions from corn stover. [c] Raw LCF solutions from wheat stover.

Table 9 Concentration of various DF solution by high-performance liquid chromatography (HPLC) with refractive index (RI) detector

Entry	Glucose (g L^{-1})	XMG[a] (g L^{-1})	Arabinose (g L^{-1})	Acetic acid (g L^{-1})	Levulinic acid (g L^{-1})	5-HMF (g L^{-1})	Furfural (g L^{-1})	Formic acid (g L^{-1})
1[a]	0.007	0.008	—	4.93	—	0.03	0.36	15.69
2[b]	0.004	—	—	9.60	—	—	0.14	13.52
3[c]	0.003	0.008	—	7.94	—	—	0.46	14.26

[a] DF solutions from red pine. [b] DF solutions from corn stover. [c] DF solutions from wheat stover.

analysis, by-products (saccharides, 5-HMF, and furfural) were no longer present in the DF solutions, which contained only organic acids (formic acid, acetic acid, and levulinic acid). This indicates that almost all the formic acid was recovered from the LCF solutions. The catalytic activity was significantly improved when the DF samples were used compared with that when the LCF solutions were used (DF from red pine: 184 mL gas production volume, 110.18% conversion, 259.09 mol H_2 mol per catalyst per h TOF (red line in Fig. 3); DF from corn stover: 170 mL gas production volume, 118.14% conversion, 109.39 mol H_2 mol per catalyst per h TOF (red line in Fig. 4); and DF from wheat stover: 167 mL gas production volume, 105.30% conversion, 103.64 mol H_2 mol per catalyst per h TOF (red line in Fig. 5)). Therefore, because the activity of the heterogeneous catalyst increases when a pure formic acid solution is used, it is necessary to develop an improved formic acid purification process for the BFH conversion process.

The gas production volume exceeded the theoretical amount in the dehydrogenation experiment using the DF solutions (over 100% conversion). According to our previous report,[48] additional formic acid was generated by the ion-exchange reaction between the additive (sodium formate) and other organic acids (acetic acid or levulinic acid).

We conducted a model experiment related to organic acid dehydrogenation. The model solution test was investigated using different model solutions of sodium formate solution (0.68 g, 15 mL), 5 mmol acetic acid without sodium formate (15 mL), 5 mmol levulinic acid without sodium formate (15 mL), 5 mmol acetic acid/sodium formate (0.68 g) (15 mL) and 5 mmol levulinic acid/sodium formate (0.68 g) (15 mL). First, we mixed the catalyst with the model solutions in a vial to visually confirm the reactivity (Fig. 7). The sodium formate solution without formic acid showed no gas generation, with only some catalyst particles moving up and down in the solution. Similarly, the organic acid solution without sodium formate exhibited no catalytic reaction. However, when an organic acid and sodium formate were mixed, vigorous gas generation was observed. We quantitatively tested various model solutions (Fig. 8). The reaction of the acetic acid model solution was completed in 60 minutes, producing a total of 170 mL of gas containing hydrogen and carbon dioxide. The levulinic acid model solution completed its reaction in 70 minutes, generating a total of 170 mL of gas. Therefore, hydrogen gas was produced from the dehydrogenation of additionally generated formic acid.

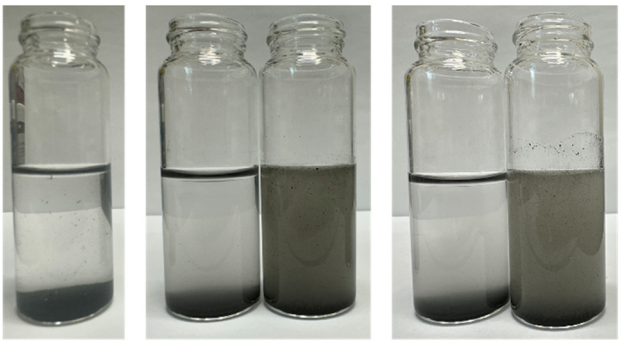

Fig. 7 Dehydrogenation catalytic reaction images (a) sodium formate reaction, (b) acetic acid reaction (left), acetic acid + sodium formate reaction (right), (c) levulinic acid reaction (left), levulinic acid + sodium formate reaction (right).

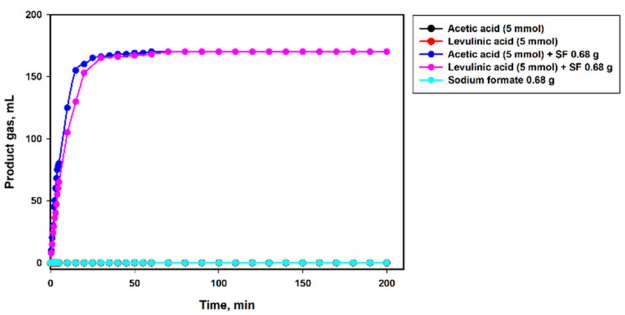

Fig. 8 Results of dehydrogenation of model solutions.

Carbon dioxide emission analysis for hydrogen production *via* the BFH conversion process

In this study, we evaluated the CO_2 emissions associated with hydrogen production from biomass and CO_2 using the BFH pathway. This process consists of three primary steps: (1) production of the CF solution from biomass *via* hydrolysis–oxidation in the presence of CO_2 and H_2O_2 solutions, (2) purification of the CF solution through distillation to obtain the DF solution, and (3) dehydrogenation of the DF solution at room temperature to produce hydrogen gas using a catalytic reaction. This analysis aimed to assess the net CO_2 reduction effect of the hydrogen production process and compare it with other hydrogen production technologies.

The detailed calculation method is described in the ESI.† First, the amount of raw material required to produce 1 ton of hydrogen was calculated. To produce 1 ton of hydrogen, the BFH process requires 67 831 kg of red pine biomass, 182 600 kg of CO_2, 476 678 kg of water, and 58 915 kg of H_2O_2. These inputs yield 22 832 kg of formic acid, which is distilled and subsequently dehydrogenated to generate 1000 kg of hydrogen (assuming 100% distillation recovery and 100% dehydrogenation yield of formic acid; the other organic acids are not considered for hydrogen production).

The CO_2 emissions were calculated for each stage of the process, assuming that the energy requirements are met by liquid natural gas (LNG) combustion. A total of 266 544 695 kcal of energy is required to produce formic acid from the red pine biomass (biomass hydrolysis–oxidation process). To meet this energy demand, 20 378 kg of LNG must be combusted. The combustion process generates 56.4 tons of CO_2. The crude formic acid solution is distilled after the hydrolysis–oxidation process, and this step requires 329 229 186 kcal of energy. The energy required for distillation is supplied by burning 25 170 kg of LNG, which emits 69.67 tons of CO_2. The dehydrogenation process is carried out at room temperature, so a heat source is not required. During the dehydrogenation process, 22 832 kg of formic acid is converted into 1000 kg of hydrogen. This chemical reaction releases 21.83 tons of CO_2. Therefore, the total CO_2 emitted during the entire BFH process is 147.9 tons.

Red pine absorbs 2.25 tons of CO_2 per ton of biomass. In this study, 67 831 kg of red pine was used, resulting in a total CO_2 absorption of 152.95 tons. Although 182 600 kg of CO_2 was used during the process, only 0.78 tons was ultimately dissolved in the reaction solution. The remaining CO_2 exists in the gas phase within the reactor system. However, this undissolved CO_2 is not vented into the atmosphere; instead, it remains within the reaction system and can be continuously cycled for reuse. This reaction system is replenished with only 0.78 ton of previously dissolved carbon dioxide. Therefore, only the CO_2 that is actually absorbed by biomass growth and reaction solution dissolution was considered in the net CO_2 reduction calculation, while the circulating CO_2 in the system was excluded from emission accounting, as it does not contribute to atmospheric release. Therefore, the total CO_2 absorption during the entire process, including both biomass growth and process utilization, was 153.73 tons.

The net CO_2 emissions of the process can be calculated by subtracting the amount of CO_2 absorbed (153.73 tons) from the total CO_2 emissions (147.9 tons), resulting in a net CO_2 reduction of 5.83 tons per ton of hydrogen produced. Additionally, 15 kg of hydrogen is produced per ton of feedstock, while −0.09 tons of CO_2 are emitted.

The net CO_2 emissions of the BFH process were compared to those in other hydrogen production pathways, as shown in Fig. 9.[73–75] The methane reforming process produces hydrogen by reacting methane with high-temperature steam, and its CO_2 emissions are calculated based on the CO_2 generated during the reaction and the CO_2 emitted from heat supply. The methane input amount and conversion efficiency relative to hydrogen production were considered. Coal gasification includes the CO_2 directly emitted from the reaction process and the CO_2 emissions from heat supply to maintain the gasification reaction temperature. The hydrogen conversion efficiency of coal gasification was taken into account. Biomass gasification accounts for CO_2 emissions from biomass transportation, direct emissions from the reaction, and CO_2 emissions from heat supply for gasification. While the net emissions are adjusted based on CO_2 absorption by biomass growth, they can vary significantly depending on the biomass feedstock and land-use change effects. For hydrogen production technologies with CCS, the CO_2 capture efficiency and energy consumption of CCS are considered. Finally, water electrolysis does not have direct CO_2 emissions, but its CO_2 footprint is calculated based on the emissions from electricity consumption. If renewable energy is used as the power source, CO_2 emissions are minimal. To maintain parallelism with relevant calculation methods, we calculated the carbon uptake of biomass, the energy usage of the process, and the direct carbon emissions during dehydrogenation. Transportation and crushing of biomass, power to operate process equipment (raw material feeders, agitators, pumps, *etc.*) are all contributing factors to carbon emissions that should be further considered in the future.

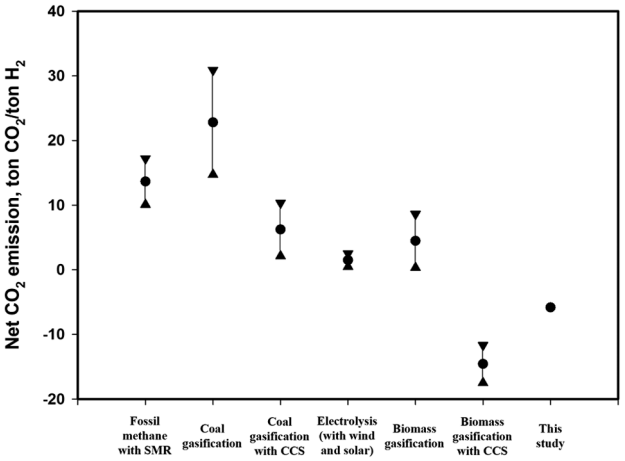

Fig. 9 Comparison of CO_2 emissions for producing 1 ton of hydrogen.

The BFH pathway significantly reduces CO_2 emissions compared to the existing hydrogen production technologies. For example, coal gasification emits between 14.72 and 30.9 tons of CO_2 per ton of hydrogen, while a net reduction of 5.83 tons was achieved in this study. Although biomass gasification combined with CCS can achieve even greater reductions, the proposed process offers a sustainable and scalable approach to hydrogen production with significant environmental benefits. These findings highlight the potential of the BFH pathway as a viable strategy for achieving carbon-neutral hydrogen production, advancing the global efforts toward sustainable energy solutions.

Conclusions

We used CO_2 as an acid reactant with H_2O_2 in the hydrolysis–oxidation process of converting biomass into formic acid. A formic acid yield of 36.18% was achieved using red pine under 30 bar CO_2 and 11 wt% H_2O_2 at 170 °C for 3 h, comparable to yields reported for conventional sulfuric acid-based processes. Our proposed process is very eco-friendly as it substitutes inorganic acids with CO_2. Formic acid yields of 17.43% and 20.45% were achieved under the same conditions using the short-lived biomass corn stover and wheat stover, respectively. By performing a structural analysis of lignocellulosic and herbaceous biomass, it was confirmed that the average molecular weight of the herbaceous biomass was much higher compared to that of the lignocellulosic biomass. Therefore, when using herbaceous biomass, more severe conditions may be required for effective formic acid conversion. Formic acid generated from various biomass sources was dehydrogenated using a heterogeneous catalyst at room temperature, and all the hydrogen conversion rates were 100%. Importantly, the process contributes to substantial carbon reduction. According to a life cycle assessment, the BFH process can achieve a net reduction of 5.83 tons of CO_2 per ton of hydrogen produced. This demonstrates the dual benefit of reducing greenhouse gas emissions while producing clean hydrogen fuel, offering a scalable and environmentally friendly solution to the challenges of the hydrogen economy. As the global demand for sustainable energy solutions grows, our method provides a feasible path towards carbon-neutral fuel production.

Author contributions

Ju-Hyoung Park: conceptualization, methodology, investigation, writing – original draft, review & editing, visualization. Young-Hoon Noh: methodology, editing. Jin Sung Kim: validation, formal analysis. Gyu-Seob Song: resources, data curation. Se-Joon Park: investigation, resources. Jong Won Choi: validation, formal analysis. Young-Chan Choi: resources, supervision. Young-Joo Lee: project administration.

Data availability

The data supporting this article have been included as part of the ESI.†

Conflicts of interest

There are no conflicts to declare.

Acknowledgements

This work was supported by the National Research Foundation of Korea (NRF) grant funded by the Korea government (MSIT) (No. 2021R1C1C2013768 (RS-2021-NR062045)).

References

1 I. Staffell, D. Scamman, A. V. Abad, P. Balcombe, P. E. Dodds, P. Ekins, N. Shah and K. R. Ward, The role of hydrogen and fuel cells in the global energy system, *Energy Environ. Sci.*, 2019, **12**, 463–491, DOI: **10.1039/C8EE01157E**.

2 Z. L. Wang, J. M. Yan, H. L. Wang, Y. Ping and Q. Jiang, Pd/C Synthesized with Citric Acid: An Efficient Catalyst for Hydrogen Generation from Formic Acid/Sodium Formate, *Sci. Rep.*, 2012, **2**(1), 598, DOI: **10.1038/srep00598**.

3 A. Bulut, M. Yurderi, Y. Karatas, M. Zahmakiran, H. Kivrak, M. Gulcan and M. Kaya, Pd-MnOx nanoparticles Dispersed on Amine-Grafted Silica: Highly Efficient Nanocatalyst for Hydrogen Production from Additive-Free Dehydrogenation of Formic Acid under Mild Conditions, *Appl. Catal., B*, 2015, **164**, 324–333, DOI: **10.1016/j.apcatb.2014.09.041**.

4 B. C. H. Steele and A. Heinzel, Materials for Fuel-Cell Technologies, *Nature*, 2001, **414**(6861), 345–352, DOI: **10.1038/35104620**.

5 M. Yurderi, A. Bulut, N. Caner, M. Celebi, M. Kaya and M. Zahmakiran, Amine Grafted Silica Supported CrAuPd Alloy Nanoparticles: Superb Heterogeneous Catalysts for the Room Temperature Dehydrogenation of Formic Acid, *Chem. Commun.*, 2015, **51**(57), 11417–11420, DOI: **10.1039/C5CC02371H**.

6 M. G. Rasul, M. A. Hazrat, M. A. Sattar, M. I. Jahirul and M. J. Shearer, The future of hydrogen: Challenges on production, storage and applications, *Energy Convers. Manage.*, 2022, **272**, 116326, DOI: **10.1016/j.enconman.2022.116326**.

7 I. Dincer and C. Acar, Review and evaluation of hydrogen production methods for better sustainability, *Int. J. Hydrogen Energy*, 2015, **40**(34), 11094–11111, DOI: **10.1016/j.ijhydene.2014.12.035**.

8 R. D. Cortright, R. R. Davda and J. A. Dumesic, Hydrogen from Catalytic Reforming of Biomass-Derived Hydrocarbons in Liquid Water, *Nature*, 2002, **418**(6901), 964–967, DOI: **10.1038/nature01009**.

9 D. Chen and L. He, Towards an Efficient Hydrogen Production from Biomass: A Review of Processes and Materials, *ChemCatChem*, 2011, **3**(3), 490–511, DOI: **10.1002/cctc.201000345**.

10 J. D. Holladay, J. Hu, D. L. King and Y. Wang, An Overview of Hydrogen Production Technologies, *Catal. Today*, 2009, **139**(4), 244–260, DOI: **10.1002/cctc.201000345**.

11 G. Iaquaniello and A. Mangiapane, Integration of Biomass Gasification with MCFC, *Int. J. Hydrogen Energy*, 2006, **31**(3), 399–404, DOI: **10.1016/j.ijhydene.2005.09.010**.

12 D. J. Wilhelm, D. R. Simbeck, A. D. Karp and R. L. Dickenson, Syngas Production for Gas-to-Liquids Applications: Technologies, Issues and Outlook, *Fuel Process. Technol.*, 2001, **71**, 139–148, DOI: **10.1016/S0378-3820(01)00140-0**.

13 J. Holladay, E. Jones, D. R. Palo, M. Phelps, Y. H. Chin, R. Dagle and E. Baker, Miniature Fuel Processors for Portable Fuel Cell Power Supplies, *MRS Online Proc. Libr.*, 2002, **756**(1), 92, DOI: **10.1557/PROC-756-FF9.2**.

14 R. M. Navarro, M. A. Peña and J. L. G. Fierro, Hydrogen Production Reactions from Carbon Feedstocks: Fossil Fuels and Biomass, *Chem. Rev.*, 2007, **107**(10), 3952–3991, DOI: 10.1021/cr0501994.

15 P. Zhang, Y. J. Guo, J. Chen, Y. R. Zhao, J. Chang, H. Junge, M. Beller and Y. Li, Streamlined hydrogen production from biomass, *Nat. Catal.*, 2018, **1**(5), 332–338, DOI: 10.1038/s41929-018-0062-0.

16 D. W. Rackemann and W. O. S. Doherty, The Conversion of Lignocellulosics to Levulinic Acid, *Biofuels, Bioprod. Biorefin.*, 2011, **5**(2), 198–214, DOI: 10.1002/bbb.267.

17 S. C. Peter, Reduction of CO_2 to Chemicals and Fuels: A Solution to Global Warming and Energy Crisis, *ACS Energy Lett.*, 2018, **3**(7), 1557–1561, DOI: 10.1021/acsenergylett.8b00878.

18 M. Ni, D. Y. C. Leung, M. K. H. Leung and K. Sumathy, An Overview of Hydrogen Production from Biomass, *Fuel Process. Technol.*, 2006, **87**(5), 461–472, DOI: 10.1016/j.fuproc.2005.11.003.

19 Y. Huang, Y. Zheng, X. Li, F. Adams, W. Luo, Y. Huang and L. Hu, Electrode Materials of Sodium-Ion Batteries toward Practical Application, *ACS Energy Lett.*, 2018, **3**(7), 1604–1612, DOI: 10.1021/acsenergylett.8b00609.

20 A. Kazim and T. N. Veziroglu, Utilization of Solar-Hydrogen Energy in the UAE to Maintain Its Share in the World Energy Market for the 21st Century, *Renewable Energy*, 2001, **24**(2), 259–274, DOI: 10.1016/S0960-1481(00)00199-3.

21 S. Van de Vyver, J. Thomas, J. Geboers, S. Keyzer, M. Smet, W. Dehaen, P. A. Jacobs and B. F. Sels, Catalytic Production of Levulinic Acid from Cellulose and Other Biomass-Derived Carbohydrates with Sulfonated Hyperbranched Poly(Arylene Oxindole)s, *Energy Environ. Sci.*, 2011, **4**(9), 3601–3610, DOI: 10.1039/C1EE01418H.

22 L. Deng, Y. Zhao, J. Li, Y. Fu, B. Liao and Q. X. Guo, Conversion of Levulinic Acid and Formic Acid into γ-Valerolactone over Heterogeneous Catalysts, *ChemSusChem*, 2010, **3**(10), 1172–1175, DOI: 10.1002/cssc.201000163.

23 M. Spangsberg, Conversion of Sugars to Lactic Acid Derivatives Using Heterogeneous Zeotype Catalysts, *Science*, 2010, **328**(5978), 602–605, DOI: 10.1126/science.118399.

24 A. Demirbaş, Biomass Resource Facilities and Biomass Conversion Processing for Fuels and Chemicals, *Energy Convers. Manage.*, 2001, **42**(11), 1357–1378, DOI: 10.1016/S0196-8904(00)00137-0.

25 J. H. Park, G. S. Song, J. S. Kim, Y. H. Noh, J. S. Park, H. Namkung, S. J. Park, J. W. Choi, D. W. Lee, Y. J. Lee and Y. C. Choi, Mechano-Noncatalytic Wet Treatment Method for Extracting Ash from Biomass at Room Temperature and Its Effect on Ash Behaviors, *ACS Sustainable Chem. Eng.*, 2023, **11**(40), 14667–14681, DOI: 10.1021/acssuschemeng.3c01913.

26 A. C. C. Chang, H. F. Chang, F. J. Lin, K. H. Lin and C. H. Chen, Biomass gasification for hydrogen production, *Int. J. Hydrogen Energy*, 2011, **36**(21), 14252–14260, DOI: 10.1016/j.ijhydene.2011.05.105.

27 J. A. Rodriguez and J. Hrbek, Interaction of Sulfur with Well-Defined Metal and Oxide Surfaces: Unraveling the Mysteries behind Catalyst Poisoning and Desulfurization, *Acc. Chem. Res.*, 1999, **32**(9), 719–728, DOI: 10.1021/ar9801191.

28 H. Kasap, D. S. Achilleos, A. Huang and E. Reisner, Photoreforming of Lignocellulose into H_2 Using Nanoengineered Carbon Nitride under Benign Conditions, *J. Am. Chem. Soc.*, 2018, **140**(37), 11604–11607, DOI: 10.1021/jacs.8b07853.

29 D. B. Pal, A. Singh and A. Bhatnagar, A review on biomass based hydrogen production technologies, *Int. J. Hydrogen Energy*, 2022, **47**(3), 1461–1480, DOI: 10.1016/j.ijhydene.2021.10.124.

30 L. Schlapbach and A. Züttel, Hydrogen-storage materials for mobile applications, *Nature*, 2001, **414**(6861), 353–358, DOI: 10.1038/35104634.

31 P. Preuster, C. Papp and P. Wasserschied, Liquid Organic Hydrogen Carriers (LOHCs): Toward a Hydrogen-free Hydrogen Economy, *Acc. Chem. Res.*, 2017, **50**(1), 74–85, DOI: 10.1021/acs.accounts.6b00474.

32 M. Niermann, S. Drunert, M. Kaltschmitt and K. Bonhoff, Liquid organic hydrogen carriers (LOHCs) – techno-economic analysis of LOHCs in a defined process chain, *Energy Environ. Sci.*, 2019, **12**(1), 290–307, DOI: 10.1039/C8EE02700E.

33 W. Wang, M. Niu, Y. Hou, W. Wu, Z. Liu, Q. Liu, S. Ren and K. N. Marsh, Catalytic conversion of biomass-derived carbohydrates to formic acid using molecular oxygen, *Green Chem.*, 2014, **16**(5), 2614–2618, DOI: 10.1039/C4GC00145A.

34 D. Teichmann, W. Arlt, P. Wasserscheid and R. Freymann, A future energy supply based on Liquid Organic Hydrogen Carriers (LOHC), *Energy Environ. Sci.*, 2011, **4**(8), 2767–2773, DOI: 10.1039/C1EE01454D.

35 H. Zhong, M. Iguchi, M. Chatterjee, Y. Himeda, Q. Xu and H. Kawanami, Formic acid-based liquid organic hydrogen carrier system with heterogeneous catalysts, *Adv. Sustainable Syst.*, 2018, **2**(2), 1700161, DOI: 10.1002/adsu.201700161.

36 A. Boddien, B. Loges, F. Gartner, C. Torborg, K. Fumino, H. Junge, R. Ludwig and M. Beller, Iron-Catalyzed Hydrogen Production from Formic Acid, *J. Am. Chem. Soc.*, 2010, **132**(26), 8924–8934, DOI: 10.1021/ja100925n.

37 F. Joó, Breakthroughs in Hydrogen Storage-Formic Acid as a Sustainable Storage Material for Hydrogen, *ChemSusChem*, 2008, **1**(10), 805–808, DOI: 10.1002/cssc.200800133.

38 Q. Y. Bi, X. L. Du, Y. M. Liu, Y. Cao, H. Y. He and K. N. Fan, Efficient Subnanometric Gold-Catalyzed Hydrogen Generation via Formic Acid Decomposition under Ambient Conditions, *J. Am. Chem. Soc.*, 2012, **134**(21), 8926–8933, DOI: 10.1021/ja301696e.

39 D. Gao, Z. Wang, C. Wang, L. Wang, Y. Chi, M. Wang, J. Zhang, C. Wu, Y. Gu, H. Wang and Z. Zhao, CrPd nanoparticles on NH_2-functionalized metal-organic framework

as a synergistic catalyst for efficient hydrogen evolution from formic acid, *Chem. Eng. J.*, 2019, **361**, 953–959, DOI: 10.1016/j.cej.2018.12.158.

40 S. Hanprerakriengkrai, H. Fujitsuka, K. Nakagawa, H. Nakagawa and T. Tago, Preparation of carbon supported Pt-Ni alloy nanoparticles catalyst with high metal loading using cation exchange resin and its application for hydrogen production, *Chem. Eng. J.*, 2019, **377**, 120276, DOI: 10.1016/j.cej.2018.10.213.

41 Q. Sun, N. Wang, Q. Wu and J. Yu, Nanopore-supported metal nanocatalysts for efficient hydrogen generation from liquid-phase chemical hydrogen storage materials, *Adv. Mater.*, 2020, **32**(44), 2001818, DOI: 10.1002/adma.202001818.

42 S. C. Huang, C. C. Cheng, Y. H. Lai and C. Y. Lin, Sustainable and selective formic acid production from photoelectrochemical methanol reforming at near-neutral pH using nanoporous nickel-iron oxyhydroxide-borate as the electrocatalyst, *Chem. Eng. J.*, 2020, **395**, 125176, DOI: 10.1016/j.cej.2020.125176.

43 S. Maerten, C. Kumpidet, D. Voß, A. Bukowski, P. Wasserscheid and J. Albert, Glucose oxidation to formic acid and methyl formate in perfect selectivity, *Green Chem.*, 2020, **22**(13), 4311–4320, DOI: 10.1039/D0GC01169J.

44 G. Centi and S. Perathoner, Opportunities and prospects in the chemical recycling of carbon dioxide to fuels, *Catal. Today*, 2009, **148**, 191–205, DOI: 10.1016/j.cattod.2009.07.075.

45 F. Proietto, U. Patel, A. Galia and O. Scialdone, Electrochemical conversion of CO_2 to formic acid using a An based electrode: A critical review on the state-of-the-art technologies and their potential, *Electrochim. Acta*, 2021, **389**, 138753, DOI: 10.1016/j.electacta.2021.138753.

46 M. Ren, H. Zheng, J. Lei, J. Zhang, X. Wang, B. I. Yakobson, Y. Yao and J. M. Tour, CO_2 to formic acid using Cu-Sn on laser-induced graphene, *ACS Appl. Mater. Interfaces*, 2020, **12**(37), 41223–41229, DOI: 10.1021/acsami.0c08964.

47 Q. Sun, B. W. J. Chen, N. Wang, Q. He, A. Chang, C. M. Yang, H. Asakura, T. Tanaka, M. J. Hulsey, C. H. Wang, J. Yu and N. Yan, Zeolite-encaged Pd-Mn nanocatalysts for CO_2 hydrogenation and formic acid dehydrogenation, *Angew. Chem., Int. Ed.*, 2020, **59**(45), 20183–20191, DOI: 10.1002/anie.202008962.

48 J. H. Park, M. H. Jin, D. W. Lee, Y. J. Lee, G. S. Song, S. J. Park, H. Namkung, K. H. Song and Y. C. Choi, Sustainable low-temperature hydrogen production from lignocellulosic biomass passing through formic acid: Combination of biomass hydrolysis/oxidation and formic acid dehydrogenation, *Environ. Sci. Technol.*, 2019, **53**(23), 14041–14053, DOI: 10.1021/acs.est.9b04273.

49 J. H. Park, D. W. Lee, M. H. Jin, Y. J. Lee, G. S. Song, S. J. Park, H. J. Jung, K. K. Oh and Y. C. Choi, Biomass-formic acid-hydrogen conversion process with improved sustainability and formic acid yield: Combination of citric acid and mechanocatalytic depolymerization, *Chem. Eng. J.*, 2021, **Part 2 421**(1), 127827, DOI: 10.1016/j.cej.2020.127827.

50 K. Tedsree, T. Li, S. Jones, C. W. A. Chan, K. M. K. Yu, P. A. J. Bagot, E. A. Marquis, G. D. W. Smith and S. C. E. Tsang, Hydrogen production from formic acid decomposition at room temperature using a Ag-Pd core-shell nanocatalyst, *Nat. Nanotechnol.*, 2011, **6**(5), 302–307, DOI: 10.1038/nnano.2011.42.

51 T. Hu, P. He, J. Wu, N. Chen, K. He, Q. Cai, R. Shen, W. Yuan, L. Zhang and X. Cao, Dehydrogenation of formic acid over ultrafine Pd particles immobilized on amine-functionalized silicon carbide, *Energy Fuels*, 2025, **39**(9), 4458–4470, DOI: 10.1021/acs.energyfuels.4c05960.

52 A. Sluiter, B. Hames, R. Ruiz, C. Scarlata, J. Sluiter and D. Templeton, Determination of Ash in Biomass. National Renewable Energy Laboratory Technical Report, 2005, NREL/TP-510-42622.

53 A. Sluiter, R. Ruiz, C. Scarlata, J. Sluiter and D. Templeton, Determination of Extractives in Biomass. National Renewable Energy Laboratory Technical Report, 2005, NREL/TP-510-42619.

54 A. Sluiter, B. Hames, R. Ruiz, C. Scarlata, J. Sluiter, D. Templeton and D. Crocker, Determination of Structural Carbohydrates and Lignin in Biomass. National Renewable Energy Laboratory Technical Report, 2008, NREL/TP-510-42618.

55 A. Sluiter, B. Hames, R. Ruiz, C. Scarlata, J. Sluiter and D. Templeton, Determination of Sugars, Byproducts, and Degradation Products in Liquid Fraction Process Samples. National Renewable Energy Laboratory Technical Report, 2006, NREL/TP-510-42623.

56 D. W. Lee, M. H. Jin, J. C. Park, C. B. Lee, D. Oh, S. W. Lee, J. W. Park and J. S. Park, Waste-Glycerol-Directed Synthesis of Mesoporous Silica and Carbon with Superior Performance in Room-Temperature Hydrogen Production from Formic Acid, *Sci. Rep.*, 2015, **5**(1), 15931, DOI: 10.1038/srep15931.

57 M. H. Jin, D. Oh, J. H. Park, C. B. Lee, S. W. Lee, J. S. Park, K. Y. Lee and D. W. Lee, Mesoporous silica supported Pd-MnOx catalysts with excellent catalytic activity in room-temperature formic acid decomposition, *Sci. Rep.*, 2016, **6**(1), 33502, DOI: 10.1038/srep33502.

58 M. H. Jin, J. H. Park, D. Oh, S. W. Lee, J. S. Park, K. Y. Lee and D. W. Lee, Pd/NH_2-KIE-6 catalysts with exceptional catalytic activity for additive-free formic acid dehydrogenation at room temperature: Controlling Pd nanoparticle size by stirring time and types of Pd precursors, *Int. J. Hydrogen Energy*, 2018, **43**(3), 1451–1458, DOI: 10.1016/j.ijhydene.2017.10.117.

59 M. H. Jin, J. H. Park, D. Oh, J. S. Park, K. Y. Lee and D. W. Lee, Effect of the amine group content on catalytic activity and stability of mesoporous silica supported Pd catalysts for additive-free formic acid dehydrogenation at room temperature, *Int. J. Hydrogen Energy*, 2019, **44**(10), 4737–4744, DOI: 10.1016/j.ijhydene.2018.12.208.

60 X. Chen, Y. Liu and J. Wu, Sustainable production of formic acid from biomass and carbon dioxide, *Mol. Catal.*, 2020, **483**, 110716, DOI: 10.1016/j.mcat.2019.110716.

61 S. Rivas, A. Raspolli Galletti, C. Antonetti, D. Licursi, V. Santos and J. Parajó, A Biorefinery cascade conversion of

hemicellulose-free Eucalyptus Globulus wood: Production of concentrated levulinic acidsolutions for γ-valerolactone sustainable preparation, *Catalysts*, 2018, **8**(4), 169, DOI: 10.3390/catal8040169.

62 D. Licursi, C. Antonetti, R. Parton and A. M. Raspolli Galletti, A novel approach to biphasic strategy for intensification of the hydrothermal process to give levulinic acid: Use of an organic nonsolvent, *Bioresour. Technol.*, 2018, **264**, 180–189, DOI: 10.1016/j.biortech.2018.05.075.

63 T. Flannelly, M. Lopes, L. Kupiainen, S. Dooley and J. J. Leahy, Non-stoichiometric formation of formic and levulinic acids from the hydrolysis of biomass derived hexose carbohydrates, *RSC Adv.*, 2016, **6**(7), 5797–5804, DOI: 10.1039/C5RA25172A.

64 F. Chambon, F. Rataboul, C. Pinel, A. Cabiac, E. Guillon and N. Essayem, Cellulose hydrothermal conversion promoted by heterogeneous bronsted and lewis acids: Remarkable efficiency of solid lewis acids to produce lactic acid, *Appl. Catal., B*, 2011, **105**, 171–181, DOI: 10.1016/j.apcatb.2011.04.009.

65 F. Jin, Z. Zhou, T. Moriya, H. Kishida, H. Higashijima and H. Enomoto, Controlling hydrothermal reaction pathways to improve acetic acid production from carbohydrate biomass, *Environ. Sci. Technol.*, 2005, **39**(6), 1893–1902, DOI: 10.1021/es048867a.

66 R. Weingarten, W. C. Conner and G. W. Huber, Production of levulinic acid from cellulose by hydrothermal decomposition combined with aqueous phase dehydration with a solid acid catalyst, *Energy Environ. Sci.*, 2012, **5**(6), 7559–7574, DOI: 10.1039/C2EE21593D.

67 K. Dussan, B. Girisuta, M. Lopes, J. J. Leahy and M. H. B. Hayes, Conversion of Hemicellulose Sugars Catalyzed by Formic Acid: Kinetics of the Dehydration of D–Xylose, L–Arabinose, and D–Glucose, *ChemSusChem*, 2015, **8**(8), 1411–1428, DOI: 10.1002/cssc.201403328.

68 R. Xing, W. Qi and W. Huber, Production of furfural and carboxylic acids from waste aqueous hemicellulose solutions from the pulp and paper and cellulosic ethanol industries, *Energy Environ. Sci.*, 2011, **4**(6), 2193–2205, DOI: 10.1039/C1EE01022K.

69 Y. Fang, X. Zeng, P. Yan, Z. Jing and F. Jin, An acidic two-step hydrothermal process to enhance acetic acid production from carbohydrate biomass, *Ind. Eng. Chem. Res.*, 2012, **51**(12), 4759–4763, DOI: 10.1021/ie202506c.

70 F. Jin, J. Yun, G. Li, A. Kishita, K. Tohji and H. Enomoto, Hydrothermal conversion of carbohydrate biomass into formic acid at mild temperatures, *Green Chem.*, 2008, **10**(6), 612–615, DOI: 10.1039/B802076K.

71 C. Wang, X. Chen, M. Qi, J. Wu, G. Gözaydın, N. Yan, H. Zhong and F. Jin, Room temperature, near-quantitative conversion of glucose into formic acid, *Green Chem.*, 2019, **21**(22), 6089–6096, DOI: 10.1039/C9GC02201E.

72 R. Sato, H. Choudhary, S. Nishimura and K. Ebitani, Synthesis of formic acid from monosaccharides using calcined Mg-Al hydrotalcite as reusable catalyst in the presence of aqueous hydrogen peroxide, *Org. Process Res. Dev.*, 2015, **19**(3), 449–453, DOI: 10.1021/op5004083.

73 L. Rosa and M. Mazzotti, Potential for hydrogen production from sustainable biomass with carbon capture and storage, *Renewable Sustainable Energy Rev.*, 2022, **157**, 112123, DOI: 10.1016/j.rser.2022.112123.

74 B. Parkinson, P. Balcombe, J. F. Speirs, A. D. Hawkes and K. Hellgardt, Levelized cost of CO_2 mitigation from hydrogen production routes, *Energy Environ. Sci.*, 2019, **12**(1), 19–40, DOI: 10.1039/C8EE02079E.

75 C. Antonini, K. Treyer, A. Streb, M. van der Spek, C. Bauer and M. Mazzotti, Hydrogen production from natural gas and biomethane with carbon capture and storage – A techno-environmental analysis, *Sustainable Energy Fuels*, 2020, **4**(6), 2967–2986, DOI: 10.1039/D0SE00222D.